Photochemical Synthesis and Structure of a 3-Dimensional Anionic Polymeric Network of an Iron(II) Oxalato Complex with Tris(2,2'-bipyridine)iron(II) Cations

Silvio Decurtins,* Helmut W. Schmalle, Philippe Schneuwly, and Hans Rudolf Oswald

Institute of Inorganic Chemistry, University of Zürich, Winterthurerstrasse 190, 8057 Zürich, Switzerland

Received October 9, 1992

The structures of single crystals of $[bipyH]^+[Fe^{III}(ox)_2(H_2O)_2]^-\cdot H_2O$ (**1**) and of a photoreaction product of **1**, namely of single crystals of a 3-dimensional polymeric compound $[Fe^{II}(bipy)_3]^{2+}{}_n[Fe^{II}{}_2(ox)_3]_n^{2n-}$ (**2**), where ox is oxalate and bipy is 2,2'-bipyridine, have been determined by X-ray diffraction. Crystal data: **1**, monoclinic, *I*1*a*1, $a = 7.302(2)$ Å, $b = 23.046(3)$ Å, $c = 10.361(2)$ Å, $\beta = 91.12(2)°$, $Z = 4$, $R(F_o) = 0.040$ for 3273 independent data [$I \geq 3\sigma(I)$]; **2**, cubic, $P4_332$, $a = 15.392(2)$ Å, $Z = 4$, $R(F_o) = 0.050$ for 1594 independent data [$I \geq 3\sigma(I)$]. $[Fe^{II}(ox)_{3/2}]^-$ units in **2** build a 3-dimensional anionic network. It can be described as a 3-connected net consisting of 10-gons, wherein the $[Fe(bipy)_3]^{2+}$ cations occupy the vacancies in an elaborate manner. There exist very few examples as yet of inorganic compounds with structures based on 3-dimensional 3-connected nets.

Introduction

The photochemistry of coordination compounds has been studied very extensively.[1,2] However there have been few reports on the use of photochemistry for the synthesis of transition metal complexes.[3] In contrast, organic or organometallic photoreactions are nowadays valuable tools in the strategy for synthesizing new and unusual molecules. Nevertheless, a photoreactive coordination compound, in which the redox reaction is combined with a change in the ligation sphere at the metallic center, can also provide a significant challenge to synthetic chemists for "molecular engineering" of new compounds.

A promising system with respect to photochemical behavior is the oxalato complexes of the transition metals M = Mn(III), Fe(III), Co(III). The oxalate ion is known to be one of the few ligands for which systematic photochemical information regarding various metal ions exists.[4-6] Oxidation-reduction is the principal photochemical reaction whereby, in the complexes of tripositive metal ions, the metal ion is reduced from the trivalent to the divalent state and the oxalate ligand is finally oxidized to carbon dioxide. In addition to its reducing property, the oxalate ion is a versatile ligand since it can act as a mono-, bi-, tri-, and tetradentate ligand capable of forming bridged polynuclear complexes.[7] Much interest exists in the oxalate ligand as a bridging unit for preparing polynuclear complexes and extended molecular assemblies in order to study magnetic ordering behavior.[8] From a structural point of view, ionic, chain, and layer structures are known. With tripositive transition metal ions, the tris chelate anions $[M^{III}(ox)_3]^{3-}$ are formed,[9,10] whereas for the dipositive transition metal ions a polymeric chain structure $[M^{II}(ox)(H_2O)_2]_n$ is predominant.[11] The structure of the lanthanide(III) oxalates typically consists of infinite layers of bridged metal oxalates, which are held together by hydrogen bonds via water molecules situated between the layers.[12] On the basis of the potential of the oxalate ion to act as a bridging ligand in forming infinite chain and layer structures, it should in principle be possible to construct a 3-dimensional network also. Now, on the basis of the photochemical reaction mechanism, a new method which directly leads to such a structure is known.

In the present paper we report our results for iron oxalato compounds. With the mononuclear tris(oxalato)ferrate(III) complex in aqueous solution at low pH, aquation reactions will first take place, whereby an oxalate ligand is replaced by two water ligands. After the addition of bipyridine to the solution, yellow crystals of the compound $[bipyH]^+[Fe^{III}(ox)_2(H_2O)_2]^-\cdot H_2O$ (**1**) can be grown with the anionic complex in a cis configuration. Of course, the cis configuration is related to the distinct crystalline state, whereas in solution a cis-trans isomerization may occur. By exposing single crystals of **1** to UV light, one observes in a short time a color change from yellow to red, starting from the surface and proceeding into the bulk. Clearly, the photoredox reaction takes place in the solid state and the Fe(II)-bipy complex is formed (red color) and CO_2 can easily be detected by IR measurements. This solid-state reaction was not pursued further. More promising has been the examination of the photoreaction of system **1** in solution. Accordingly, the yellow solution of **1** also turns red by exposure to UV light, indicating the formation of $[Fe^{II}(bipy)_3]^{2+}$ cations, and red single crystals in at least three different modifications can be grown. One form, which is insoluble in H_2O, turned out to belong to the cubic crystal system and is based on a structure consisting of a 3-dimensional $[Fe^{II}{}_2(ox)_3]_n^{2n-}$ network with n $[Fe^{II}(bipy)_3]^{2+}$ cations (**2**). The structures of **1** and **2** will be discussed. The structure determinations of the other modifications are still in progress.

As a matter of fact, the combined action of photoreducing the iron(III) oxalato complex to the iron(II) state while offering a cation suitable in charge, size, and symmetry for crystallization enables the system to form this new 3-dimensional network.

Experimental Section

Synthesis of $[bipyH]^+[Fe^{III}(ox)_2(H_2O)_2]^-\cdot H_2O$ (1). All chemicals were of reagent grade and were used as commercially obtained. $K_3[Fe(ox)_3]\cdot 3H_2O$ was prepared according to literature methods.[13] To a 0.1 *m* aqueous solution of the tris(oxalato)ferrate(III) complex was added

* Author to whom correspondence should be addressed.

(1) Balzani, V.; Carassiti, V. *Photochemistry of Coordination Compounds*; Academic Press: London, 1970.
(2) Adamson, A. W., Fleischauer, P. D., Eds. *Concepts of Inorganic Photochemistry*; Wiley: New York, 1975.
(3) Sykora, J.; Sima, J. *Coord. Chem. Rev.* **1990**, *107*, 1.
(4) Porter, G. B.; Doering, J. G. W.; Karanka, S. *J. Am. Chem. Soc.* **1962**, *84*, 4027.
(5) Wehry, E. L. *Q. Rev., Chem. Soc.* **1967**, *21*, 213.
(6) Simmons, E. L.; Wendlandt, W. W. *Coord. Chem. Rev.* **1971**, *7*, 11.
(7) Scott, K. L.; Wieghardt, K.; Sykes, A. G. *Inorg. Chem.* **1973**, *12*, 655.
(8) Oshio, H.; Nagashima, U. *Inorg. Chem.* **1992**, *31*, 3295.
(9) Herpin, P. *Bull. Soc. Fr. Mineral. Cristallogr.* **1958**, *81*, 245.
(10) Merrachi, E. M.; Mentzen, B. F.; Chassagneux, F.; Bouix, J. *Rev. Chim. Miner.* **1987**, *24*, 56.
(11) Deyrieux, R.; Peneloux, A. *Bull. Soc. Chim. Fr.* **1969**, *8*, 2675.
(12) Birnbaum, E. R. In *Gmelin Handbook of Inorganic Chemistry*; Moeller, T.; Schleitzer-Rust, E., Eds.; Springer Verlag: Berlin, 1984; Vol. 39 (D5), p 112.

0020-1669/93/1332-1888$04.00/0

Table I. Crystal Data and Structure Determination Parameters

	$[bipyH]^+[Fe^{III}(ox)_2(H_2O)_2]^-\cdot H_2O$	$[Fe^{II}(bipy)_3]^{2+}{}_n[Fe^{II}_2(ox)_3]_n^{2n-}$
formula	$C_{14}H_{15}N_2O_{11}Fe$	$C_{36}H_{24}N_6O_{12}Fe_3$
fw	443.13	900.17
temp, K	296	296
cryst system	monoclinic	cubic
space group	*Ia* (No. 9)	$P4_332$ (No. 212)
a, Å	7.302(2)	15.392(2)
b, Å	23.046(3)	
c, Å	10.361(2)	
β, deg	91.12(2)	
V, Å^3	1743(1)	3647(1)
Z	4	4
calcd density, g cm^{-3}	1.69	1.64
obsd density, g cm^{-3}	1.69	1.63
color, habit	yellow, prism	deep red, regular octahedron
cryst size, mm	0.26 × 0.04 × 0.25	edge length 0.32
μ(Mo Kα), cm^{-1}	9.25	12.31
F(000)	908	1824
$R(F_o)^a$	0.040	0.050
$R_w(F_o)^a$	0.028	0.033
w	$1.398/\sigma^2(\lvert F_o\rvert)$	$3.511/\sigma^2(\lvert F_o\rvert)$

^{a} $R = \sum(\lvert F_o\rvert - \lvert F_c\rvert)/\sum\lvert F_o\rvert$. $R_w = [(\sum w\lvert F_o\rvert - \lvert F_c\rvert)^2/\sum w\lvert F_o^2\rvert]^{0.5}$.

nitric acid to achieve a pH value of 1–2. A color change from green to yellow was observed, indicating the formation of the $[Fe^{III}(ox)_2(H_2O)_2]^-$ anion. Bipyridine (1 equiv) was added, and slow evaporation of this solution in the dark yielded yellow, elongated prismatic crystals of **1**. Anal. Calcd for $C_{14}H_{15}N_2O_{11}Fe$: C, 37.9; H, 3.4; N, 6.3. Found: C, 38.4; H, 3.4; N, 6.1.

Synthesis of $[Fe^{II}(bipy)_3]^{2+}{}_n[Fe^{II}_2(ox)_3]_n^{2n-}$ (2). Following the preparation method for **1**, the final solution was exposed to UV light (366 nm) for about 15 min. The solution turned red instantaneously, indicating the reduction of the iron(III) to the divalent state and the formation of the Fe(II)–bipy complex. Slow evaporation of this solution yielded red crysals in three different modifications: hexagonal plates, prismatic crystals of the monoclinic system, and cubic crystals with an octahedral habit, **2**. Anal. Calcd for $C_{36}H_{24}N_6O_{12}Fe_3$: C, 48.0; H, 2.7; N, 9.3. Found (microcrystalline precipitate): C, 47.8; H, 2.9; N, 9.0.

X-ray Crystallographic Analysis. Relevant crystallographic data and structure determination parameters for the two compounds are given in Tables I and SVIII (supplementary material). Cell parameters were derived from precession photographs and refined by the least-squares method with 25 reflections [7.6° < θ < 12.4° (**1**) and 8.4° < θ < 11.4° (**2**)] carefully centered on the diffractometer. Intensity data for the iron(II) and iron(III) complexes were measured at room temperature on an Enraf-Nonius CAD-4 diffractometer with graphite-monochromated Mo Kα radiation (λ = 0.710 73 Å). The ω–2θ scan technique with variable scan speeds of 1.65–16.5° min^{-1} for **1** and 1.27–3.49° min^{-1} for **2** was used. Three standard reflections were measured at an interval of every 3 h for **1** and **2**. For compound **1** a decay of 3.8% during data collection was observed and corrected for in data reduction, whereas for **2** no significant decrease in intensities was noted. To control orientation, three reflections were checked every 400 reflections in both data collections. Numerical absorption corrections based on seven (**1**) and eight (**2**) crystal faces and Lorentz and polarization corrections were applied to the data. The structures were solved by Patterson syntheses with SHELXS86[14] and refined with SHELX76.[15] Least-squares refinements were carried out by minimizing $\sum w(\lvert F_o\rvert - \lvert F_c\rvert)^2$ with $w = 1.398/\sigma^2(F_o)$ (**1**) and $w = 3.511/\sigma^2(F_o)$ (**2**). All non-hydrogen atoms in both structures were refined with anisotropic displacement parameters. All hydrogen atoms were localized in difference electron density maps and refined with variable positional and isotropic displacement parameters for the monoclinic structure (**1**) and also for the cubic structure (**2**).

Table II. Positional and Equivalent Isotropic Displacement Parameters for $[bipyH]^+[Fe^{III}(C_2O_4)_2(H_2O)_2]^-\cdot H_2O$ (**1**)

atom	*x*/*a*	*y*/*b*	*z*/*c*	U_{eq},^{a} Å^2
Fe(1)	0.0000	0.13471(2)	0.0000	0.02360(8)
O(11)	0.9510(4)	0.0685(1)	0.8823(2)	0.0317(5)
O(21)	0.9656(3)	0.0746(1)	1.1314(2)	0.0302(5)
O(31)	0.8852(4)	−0.0189(1)	1.1503(3)	0.0495(6)
O(41)	0.8856(4)	−0.0258(1)	0.8838(3)	0.0469(6)
C(11)	0.9181(5)	0.0201(2)	0.9396(3)	0.0292(5)
C(21)	0.9214(5)	0.0240(2)	1.0870(3)	0.0306(5)
O(12)	0.9884(4)	0.1916(1)	0.8510(2)	0.0313(5)
O(22)	0.7316(3)	0.1588(1)	1.0073(2)	0.0297(5)
O(32)	0.7917(4)	0.2499(1)	0.7444(3)	0.0528(5)
O(42)	0.5162(3)	0.2052(1)	0.8950(3)	0.0469(5)
C(12)	0.8303(5)	0.2137(2)	0.8275(4)	0.0337(6)
C(22)	0.6777(5)	0.1910(1)	0.9175(3)	0.0267(5)
O(W1)	1.2718(3)	0.1265(1)	0.9835(3)	0.0363(6)
O(W2)	1.0583(4)	0.1979(1)	1.1283(3)	0.0393(6)
N(1)	0.7374(5)	0.0529(2)	0.4014(3)	0.0459(6)
C(2)	0.7321(6)	0.1101(2)	0.4020(5)	0.0609(6)
C(3)	0.6756(7)	0.1422(2)	0.5042(6)	0.0699(7)
C(4)	0.6215(7)	0.1128(2)	0.6127(5)	0.0732(7)
C(5)	0.6259(6)	0.0532(2)	0.6169(4)	0.0550(7)
C(6)	0.6848(5)	0.0248(2)	0.5058(4)	0.0387(6)
N(2)	0.7473(4)	−0.0591(1)	0.3811(3)	0.0358(5)
C(2a)	0.7560(6)	−0.1153(2)	0.3562(4)	0.0478(6)
C(3a)	0.7063(6)	−0.1563(2)	0.4440(4)	0.0543(6)
C(4a)	0.6474(6)	−0.1364(2)	0.5626(4)	0.0600(6)
C(5a)	0.6379(6)	−0.0781(2)	0.5897(4)	0.0493(7)
C(6a)	0.6881(5)	−0.0382(2)	0.4945(4)	0.0365(6)
O(W3)	0.3960(4)	0.2298(2)	0.1792(3)	0.0801(7)

^{a} $U_{eq} = {}^1/_3\sum_i\sum_j U_{ij}a^*_i a^*_j \mathbf{a}_i\cdot\mathbf{a}_j$.

Results and Discussion

$[bipyH]^+[Fe^{III}(ox)_2(H_2O)_2]^-\cdot H_2O$ (1). Our interest in a structural characterization of this compound stems from the fact that it represents the educt side of the photochemical reaction path. The anionic complex results from an aquation reaction which takes place in acidic solution,[16] but the only structural verification so far has been in the case of the chromium(III) compound.[17] Bipyridine, added to the solution in order to act as a second ligand during the photoredox reaction, serves in the protonated form as an appropriate cation for crystallization.

The structure is noncentrosymmetric. According to the choice of the cell axes, systematic extinctions for a body-centered cell indicate possible space groups *I*2/*a* (No. 15) and *Ia* (No. 9). *E* statistics[18] and *N*(*Z*) tests,[19] carried out with all 6397 [including 3124 unobserved with $I < 3\sigma(I)$] measured reflections, clearly favor the noncentrosymmetric space group *Ia*. The noncentrosymmetric structure and its inversion were refined successfully using the complete data set of all observed reflections and 315 variable parameters. The final R/R_w values for the structure presented here were calculated to be 3.96/2.84%, and those for its inversion, to be 4.27/3.17%. $\Delta R_w = 0.33$ and the presented structure is significant at the 0.005 level when Hamilton's *R* factor test[20] is applied. Final positional and equivalent isotropic displacement parameters are given in Tables II and SIX (supplementary material).

A thermal ellipsoid plot of the chiral anion, which crystallizes in the cis configuration, is depicted in Figure 1. Interatomic distances and angles are collected in Tables III and IV. The oxalate ligands are planar and have no significant deformation on forming the chelate rings. Figure 2[21] represents a projection

(13) Bailar, J. C.; Jones, E. M. In *Inorganic Syntheses*; Booth, H. S., Ed.; McGraw-Hill Book Co.: New York, 1939; Vol. 1, p 35.
(14) Sheldrick, G. M. SHELXS86, Crystal Structure Solution. In *Crystallographic Computing*; Sheldrick, G. M., Krüger, C., Goddard, R., Eds.; Oxford University Press: Oxford, England, 1985; p 175.
(15) Sheldrick, G. M. SHELX76. Program for Crystal Structure Determination. University of Cambridge, Cambridge, England, 1976.
(16) Krishnamurty, K. V.; Harris, G. M. *Chem. Rev.* **1961**, *61*, 213.
(17) Niekerk, J. N.; Schoening, F. R. L. *Acta Crystallogr.* **1951**, *4*, 35.
(18) Karle, I. L.; Dragonette, K. S.; Brenner, S. A. *Acta Crystallogr.* **1965**, *19*, 713.
(19) Howells, E. R.; Phillips, D. C.; Rogers, D. *Acta Crystallogr.* **1950**, *3*, 210.
(20) Hamilton, W. C. *Acta Crystallogr.* **1965**, *18*, 502.
(21) Keller, E. SCHAKAL86: A Fortran Program for the Graphic Representation of Molecular and Crystallographic Models. *Chem. Unserer Zeit* **1986**, *20*, 178.

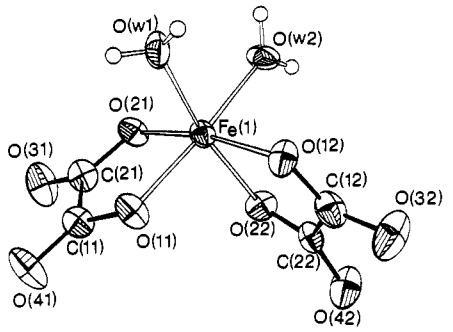

Figure 1. ORTEP drawing (50% probability) of the *cis*-$[Fe^{III}(ox)_2(H_2O)_2]^-$ anion of compound **1**.

Table III. Bond Distances (Å) for $[bipyH]^+[Fe^{III}(C_2O_4)_2(H_2O)_2]^-\cdot H_2O$ (**1**)

Fe(1)–O(11)	1.982(3)	Fe(1)–O(12)	2.026(3)
Fe(1)–O(21)	1.962(2)	Fe(1)–O(22)	2.039(2)
Fe(1)–O(W1)	2.004(2)	Fe(1)–O(W2)	2.011(3)
N(1)–C(2)	1.319(5)	N(1)–C(6)	1.324(4)
C(2)–C(3)	1.362(6)	C(3)–C(4)	1.377(7)
C(4)–C(5)	1.374(7)	C(5)–C(6)	1.400(5)
N(2)–C(2a)	1.323(5)	N(2)–C(6a)	1.349(4)
C(2a)–C(3a)	1.366(5)	C(3a)–C(4a)	1.388(6)
C(4a)–C(5a)	1.375(6)	C(5a)–C(6a)	1.401(5)
C(6)–C(6a)	1.457(4)		
C(11)–O(11)	1.289(4)	C(11)–O(41)	1.225(4)
C(21)–O(21)	1.293(4)	C(21)–O(31)	1.218(4)
C(12)–O(12)	1.281(4)	C(12)–O(32)	1.228(4)
C(22)–O(22)	1.248(4)	C(22)–O(42)	1.241(4)
C(11)–C(21)	1.529(4)	C(12)–C(22)	1.557(5)

Table IV. Bond Angles (deg) for $[bipyH]^+[Fe^{III}(C_2O_4)_2(H_2O)_2]^-\cdot H_2O$ (**1**)

O(11)–Fe(1)–O(21)	81.9(1)	O(11)–Fe(1)–O(12)	91.4(1)
O(12)–Fe(1)–O(21)	169.1(1)	O(11)–Fe(1)–O(22)	94.0(1)
O(21)–Fe(1)–O(22)	91.7(1)	O(12)–Fe(1)–O(22)	80.0(1)
O(11)–Fe(1)–O(W1)	92.4(1)	O(12)–Fe(1)–O(W1)	91.3(1)
O(21)–Fe(1)–O(W1)	97.6(1)	O(22)–Fe(1)–O(W1)	169.3(1)
O(11)–Fe(1)–O(W2)	175.9(1)	O(12)–Fe(1)–O(W2)	92.3(1)
O(21)–Fe(1)–O(W2)	94.6(1)	O(22)–Fe(1)–O(W2)	88.3(1)
O(W1)–Fe(1)–O(W2)	85.9(1)	C(11)–O(11)–Fe(1)	114.6(2)
C(21)–O(21)–Fe(1)	115.1(2)	C(12)–O(12)–Fe(1)	115.2(2)
C(22)–O(22)–Fe(1)	115.1(1)		
C(2)–N(1)–C(6)	118.5(4)	N(1)–C(2)–C(3)	123.7(5)
C(2)–C(3)–C(4)	117.7(4)	C(3)–C(4)–C(5)	120.7(4)
C(4)–C(5)–C(6)	116.7(4)	N(1)–C(6)–C(5)	122.8(4)
N(1)–C(6)–C(6a)	114.7(3)	C(5)–C(6)–C(6a)	122.5(4)
C(2a)–N(2)–C(6a)	122.4(3)	N(2)–C(2a)–C(3a)	122.3(4)
C(2a)–C(3a)–C(4a)	116.8(4)	C(3a)–C(4a)–C(5a)	121.5(4)
C(4a)–C(5a)–C(6a)	118.8(4)	N(2)–C(6a)–C(5a)	118.2(4)
N(2)–C(6a)–C(6)	115.5(3)	C(5a)–C(6a)–C(6)	126.3(4)
O(11)–C(11)–C(21)	114.2(3)	O(11)–C(11)–O(41)	124.4(3)
C(21)–C(11)–O(41)	121.4(3)	O(21)–C(21)–C(11)	114.1(3)
O(21)–C(21)–O(31)	126.6(3)	C(11)–C(21)–O(31)	119.4(3)
O(12)–C(12)–O(32)	126.7(3)	O(12)–C(12)–C(22)	113.9(3)
C(22)–C(12)–O(32)	119.4(3)	O(22)–C(22)–O(42)	125.6(3)
C(12)–C(22)–O(22)	115.3(3)	C(12)–C(22)–O(42)	119.2(3)

of the crystal structure onto the *bc* plane. The complex anions form a framework, stabilized, on the one hand, by intermolecular hydrogen-bonding contacts mainly between coordinated water as donors and oxalate oxygens as acceptors (Table V) and, on the other hand, by stacking interactions (mean stacking distance 3.28 Å) between C(11)-oxalate groups. The bipyridinium cations, occupying the holes of the framework, are strictly planar [maximum deviation from a least-squares plane defined by all bipy atoms is 0.038 Å for C(3)]. The NH proton was localized in the electron density map at both N(1) and N(2) positions and was refined with site occupation factors of 0.5 for each one. An intramolecular hydrogen bond of the form N–H···N stabilizes the planar conformation of the cation (Table V). The mean

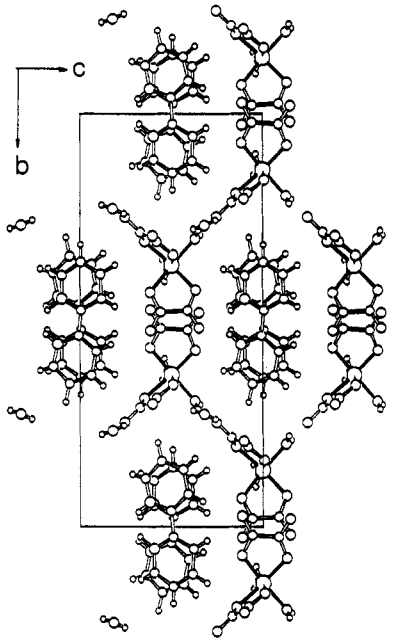

Figure 2. Molecular arrangement of compound **1** shown in the *bc* plane.

Table V. Hydrogen-Bonding Contacts for $[bipyH]^+[Fe^{III}(C_2O_4)_2(H_2O)_2]^-\cdot H_2O$ (**1**)[a]

X–H···Y	X–H, Å	H···Y, Å	X···Y, Å	X–H···Y, deg
N(1)–H(1N)···O(31^{i})	1.10(2)	2.19(2)	3.283(4)	170(2)
N(2)–H(2N)···O(31^{i})	0.87(3)	2.07(2)	2.772(4)	138(2)
N(2)–H(2N)···N(1)	0.87(3)	2.21(3)	2.591(5)	106(2), intra
C(5a)–H(5a)···O(11^{ii})	0.95(2)	2.51(2)	3.356(5)	149(2)
O(W1)–H(W11)···O(41^{iii})	0.80(2)	1.87(2)	2.680(4)	172(2)
O(W1)–H(W12)···O(42^{iv})	0.74(2)	1.99(2)	2.716(4)	167(2)
O(W2)–H(W21)···O(32^{v})	0.68(2)	1.97(2)	2.603(4)	157(3)
O(W2)–H(W22)···O(W3^{vi})	0.82(1)	1.81(1)	2.618(4)	166(2)
O(W3)–H(W31)···O(42^{i})	0.78(2)	2.41(2)	3.141(4)	157(2)
O(W3)–H(W32)···O(42^{vii})	0.73(2)	2.10(2)	2.817(4)	167(3)

[a] Symmetry operations: i = $x, y, -1 + z$; ii = $-0.5 + x, -y, z$; iii = $0.5 + x, -y, z$; iv = $1 + x, y, z$; v = $x, 0.5 - y, 0.5 + z$; vi = $1 + x, y, 1 + z$; vii = $x, 0.5 - y, -0.5 + z$.

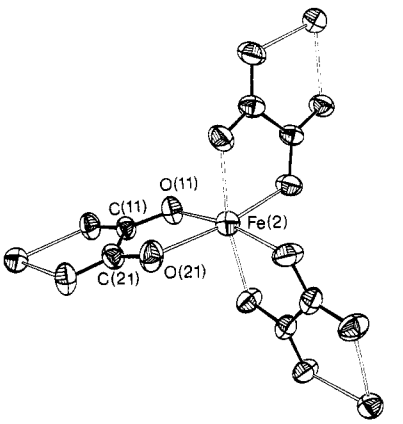

Figure 3. ORTEP drawing (50% probability) of the Fe(2) coordination in the 3-dimensional Fe–oxalato network (**2**).

value of the stacking distance between the bipyridinium cations is 3.41 Å (symmetry operation $0.5 + x, -y, z$).

$[Fe^{II}(bipy)_3]^{2+}{}_n[Fe^{II}_2(ox)_3]_n^{2n-}$ (2), a product of a photoredox reaction of an aqueous solution of compound **1**, exhibits a remarkable structure. It forms a 3-dimensional (3D), polymeric anionic network with the tris-chelated cations occupying the vacancies of the framework. Figure 3 shows a thermal ellipsoid plot of the Fe(2) coordination in the 3D Fe–oxalato network. The oxalate ligands repeatedly bridge adjacent Fe(2) ions in all three

Table VI. Positional Parameters, Site Occupation Factors (Sof's), Wyckoff Notation, and Equivalent Isotropic Displacement Parameters for $[Fe^{II}(bipy)_3]^{2+}{}_n[Fe^{II}_2(C_2O_4)_3]_n^{2n-}$ (**2**)

atom	x/a	y/b	z/c	sof	Wyck	U_{eq}/U_{iso}[a] Å^2
Fe(1)	0.1250	0.1250	0.1250	1/6	a	0.02130(8)
Fe(2)	0.35255(3)	0.35255(3)	0.35255(3)	1/3	c	0.03610(8)
O(11)	0.4896(1)	0.3398(1)	0.3649(2)	1.0	e	0.0383(5)
O(21)	0.3661(1)	0.2155(1)	0.3592(2)	1.0	e	0.0426(5)
C(11)	0.5133(2)	0.2633(2)	0.3750	0.5	d	0.0292(7)
C(21)	0.4419(2)	0.1919(2)	0.3750	0.5	d	0.0335(7)
N(1)	0.2529(1)	0.1157(2)	0.1250(2)	1.0	e	0.0266(5)
C(2)	0.3096(2)	0.1814(2)	0.1274(2)	1.0	e	0.0397(6)
C(3)	0.3988(2)	0.1680(3)	0.1302(3)	1.0	e	0.0518(7)
C(4)	0.4304(2)	0.0855(3)	0.1296(3)	1.0	e	0.0527(8)
C(5)	0.3728(3)	0.0171(2)	0.1270(2)	1.0	e	0.0422(7)
C(6)	0.2839(2)	0.0326(2)	0.1255(2)	1.0	e	0.0282(6)
H(2)	0.2878(14)	0.2381(14)	0.1239(15)	1.0	e	0.031(3)
H(3)	0.4340(15)	0.2139(16)	0.1317(17)	1.0	e	0.044(3)
H(4)	0.4897(15)	0.0702(15)	0.1341(16)	1.0	e	0.048(3)
H(5)	0.3881(15)	−0.0321(14)	0.1275(15)	1.0	e	0.024(3)

[a] $U_{eq} = {}^1/_3\sum_i\sum_j U_{ij}a^*_i a^*_j \mathbf{a}_i\cdot\mathbf{a}_j$.

Table VII. Bond Distances (Å) and Angles (deg) for $[Fe^{II}(bipy)_3]^{2+}{}_n[Fe^{II}_2(C_2O_4)_3]_n^{2n-}$ (**2**)

Fe(1)–N(1)	1.973(2) (6×)	Fe(2)–O(11)	2.128(2) (3×)
		Fe(2)–O(21)	2.122(2) (3×)
N(1)–C(2)	1.338(4)	N(1)–C(6)	1.364(4)
C(2)–C(3)	1.389(4)	C(3)–C(4)	1.360(5)
C(4)–C(5)	1.378(5)	C(5)–C(6)	1.391(5)
C(6)–C(6a)	1.447(5)		
C(11)–O(11)	1.242(3) (2×)	C(21)–O(21)	1.246(3) (2×)
C(11)–C(21)	1.555(6)		
N(1)–Fe(1)–N(1)	94.2(1) (6×)	N(1)–Fe(1)–N(1)	81.7(1) (3×)
N(1)–Fe(1)–N(1)	90.3(2) (3×)	N(1)–Fe(1)–N(1)	174.1(1) (3×)
C(6)–N(1)–Fe(1)	114.6(2)	C(2)–N(1)–Fe(1)	126.6(2)
O(11)–Fe(2)–O(11)	90.6(1) (3×)	O(11)–Fe(2)–O(21)	78.8(1) (3×)
O(11)–Fe(2)–O(21)	92.9(1) (3×)	O(11)–Fe(2)–O(21)	168.9(1) (3×)
O(21)–Fe(2)–O(21)	98.1(1) (3×)	C(11)–O(11)–Fe(2)	112.9(2)
C(21)–O(21)–Fe(2)	113.1(2)		
C(6)–N(1)–C(2)	118.7(2)	N(1)–C(2)–C(3)	122.3(3)
C(2)–C(3)–C(4)	119.5(3)	C(3)–C(4)–C(5)	118.9(3)
C(4)–C(5)–C(6)	120.2(3)	C(5)–C(6)–N(1)	120.4(3)
N(1)–C(6)–C(6a)	114.5(2)	C(5)–C(6)–C(6a)	125.1(2)
O(11)–C(11)–O(11)	124.8(3)	O(11)–C(11)–C(21)	117.6(2)
O(21)–C(21)–O(21)	125.8(3)	C(11)–C(21)–O(21)	117.1(2)

dimensions, which finally leads to a polymeric net. Looked upon as a fragmental tris(oxalato)–iron(2) unit, it possesses a D_3 point group symmetry and the same holds for the tris(bipyridine)–iron(1) cations. A tris(bidentate ligand) complex may be described as a "trigonally distorted octahedron". It is of interest to describe the nature of this distortion in more detail.[22] An octahedron, viewed along a C_3 axis, exhibits two perfectly staggered equilateral triangles of site s, which are exactly $h = (2/3)^{1/2}s$ apart. Distortions which lower the point symmetry from O_h to D_3 can be described with two parameters: an angle ϕ for the twisting of the triangles with respect to each other (60° for a regular octahedron) and the ratio s/h, describing the degree of compression or elongation with respect to the regular octahedron, which is $s/h = 1.22$. The tris(oxalato)–iron(2) complex must be described by a twist angle of 48° and an s/h ratio of 1.42 (s = 3.205(4) Å, h = 2.253 Å), which corresponds to a slightly twisted and compressed octahedron.

The structure is determined to be noncentrosymmetric. Possible space groups are $P4_332$ (No. 212) and $P4_132$ (No. 213), because hkl values are cyclically permutable and the reflection conditions for $h00$ are $h = 4n$. The structure can be solved in the space groups $P4_132$ or $P4_332$ and $P2_12_12_1$; the latter was used to achieve better 3-dimensional information for an initial graphical inter-

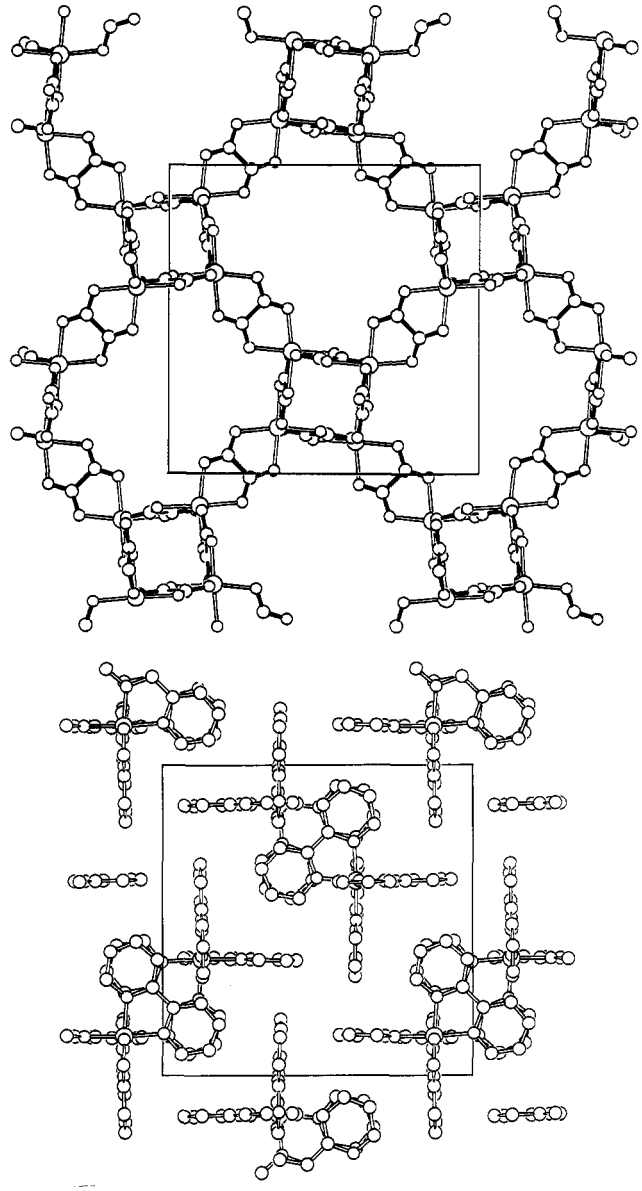

Figure 4. [100] projections of (a, top) $[Fe^{II}_2(ox)_3]_n^{2n-}$ and (b, bottom) $[Fe^{II}(bipy)_3]^{2+}$ for compound **2**.

pretation of the new structure. A first measured crystal, probably merohedrically twinned, revealed a lower R_w value in space group $P4_132$, whereas the presented data from a refinement with a second measured crystal show the clear preference for space group $P4_332$. The structure was finally refined with constrained positional parameters for C(11) and C(21) of the oxalate group, lying on a 2-fold axis ($-y$, $^3/_4 + y$, $^3/_8$ in space group $P4_132$ and y, $^1/_4 - y$, $^5/_8$ in space group $P4_332$), using 1594 observed reflections and 104 variable paramters. The R/R_w values for the different enantiomorphs were calculated to be 5.79/3.83% and 5.03/3.27%. Thus the enantiomorph with the lower R value (in space group $P4_332$) was chosen for the final calculations. The final maximum and minimum residual electron density values are 2.82 e Å^{-3} [0.13 Å from Fe(1)]; the second highest electron density peaks appeared to be 0.96 e Å^{-3} (see discussion below) and −0.87 e Å^{-3} [0.46 Å from Fe(1)]. Final positional and equivalent isotropic displacement parameters are given in Table VI, and bond distances and angles are shown in Table VII. The $Fe^{II}(2)$–O(11)/O(21) bond distances are significantly longer (mean value 0.12 Å) than the corresponding $Fe^{III}(1)$–oxygen bond distances of compound **1** (Table III). The values for the oxalate ligands can be compared with the results of a recent high-resolution X-ray diffraction study

(22) Stiefel, E. I.; Brown, G. F. *Inorg. Chem.* **1972**, *11*, 434.

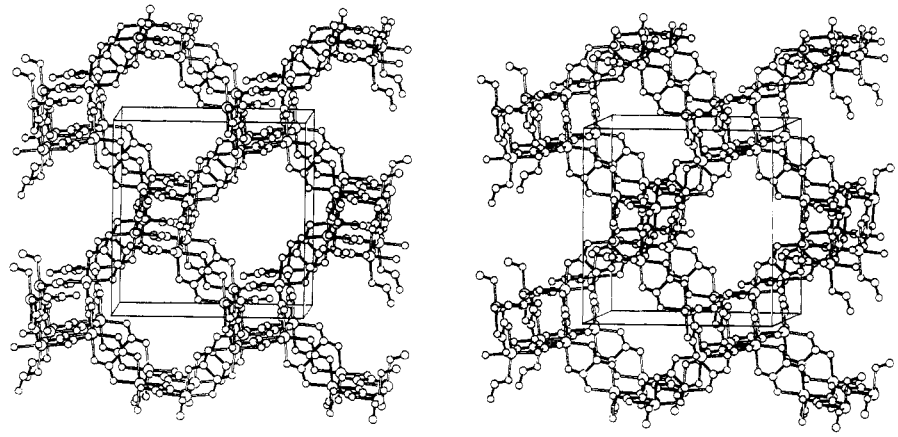

Figure 5. Stereoview of a section of the 3-dimensional $[Fe^{II}_2(ox)_3]_n^{2n-}$ network (**2**).

of oxalic acid.[23] If any, only one hydrogen interaction of the type C–H···O can be observed in compound **2**: distances C(4)–H(4) = 0.94(2), H(4)···O(11) = 2.59(2), C(4)···O(11) = 3.510(4) Å; angle C(4)–H(4)···O(11) = 165(2)°; symmetry operation $z, -1 + x, y$.

In space group $P4_332$, Fe(2) is chelated by the oxalate ligands in the Δ configuration (accordingly, in the Λ configuration for space group $P4_132$) and it occupies the site with symmetry 3 (Wyckoff letter c). The Fe(1)–bipyridine complex unambiguously appears to also have the Δ configuration and Fe(1) occupies the site with symmetry 32 (Wyckoff letter a). In the final difference Fourier map, the second highest residual electron density peak (0.96 e Å^{-3}) was found on the position $^5/_8$, $^5/_8$, $^5/_8$, which corresponds also to the site with symmetry 32 but to the Wyckoff letter b. From least-squares distance, and angle calculations it is revealed that an occupation of the b site by Fe(1), as judged by geometrical considerations, is in principle possible with coordinated bipy molecules in the Λ configuration. However, test calculations with the Δ configuration of the oxalate net and the Λ configuration of the bipy complex resulted in poor convergence, giving non-positive definite displacement parameters for Fe(1) and most of the bipyridine atoms. This clearly demonstrates the preference for the Δ–Δ combination in space group $P4_332$. A mixed occupation of both a and b sites, using Δ and Λ configurations of the cations in the least-squares calculations, is prohibited because of space-filling restrictions.

Figure 4 shows [100] projections of the $[Fe^{II}_2(ox)_3]_n^{2n-}$ net and the $[Fe^{II}(bipy)_3]^{2+}$ cations. From the former, it can be seen that the net forms 4-fold helices which all will turn clockwise upward (anticlockwise in space group 4_132). This 4-fold symmetry is also adopted by the cation arrangement within the anionic framework. The bridging oxalate ligands are planar [maximum deviation from a least-squares plane defined by the symmetry-independent atoms C(11), C(21), O(11), and O(21) is 0.019 Å for C(11)]. According to symmetry, only half of the bipyridine defines a least-squares plane with maximum out-of-plane deviation of 0.007 Å for C(6).

In Figure 5, a stereoplot of the anionic network is given. This view reveals a complementary aspect of the structural connections within the framework. In a formalistic way,[24] it can be described as a cubic 3-connected 10-gon net (10,3) and it may be considered as the 3-connected analogue of the diamond net. The $[Fe^{II}(ox)_{3/2}]^-$ units are the 3-connected points and four of them together (Z = 4) have the necessary number (6) of free links to build the 3D net. Identically oriented links repeat at intervals of (Z + 1) points, so that circuits of 2(Z + 1) points are formed. The structure represents a uniform net in the sense that the shortest path, starting from any point along any link and returning to that point along any other link, is a circuit of 10 points.

Discussing the aspect of the spin states of the iron in both complexes of compound **2**, it is generally known, that iron(II) in the tris(bipyridine) complex possesses a low-spin-state configuration. At the same time, in the tris(oxalato)iron(II) complexes, the iron will be in the high-spin state.[25]

With regard to the mechanistic pathway which leads to the structure of compound **2**, our knowledge is far from complete. The photoredox reaction of the tris(oxalato)ferrate(III) ion normally leads to the known chain structure of the divalent metal oxalato compounds. In the present case, the additional interfering effect of the bipyridine ligand during the photoredox process suppresses the formation of the linear structure. At the same time, the $[Fe^{II}(bipy)_3]^{2+}$ cations which are formed during the redox process represent just the suitable counterions needed to fill the vacancies in the open anionic network. They turn out to be adequate with respect to charge, size, and symmetry while occupying the available four special positions of the underlying space group.

As an outlook, further experiments with a variation of the metal ion [Mn(III), Co(III)] and of the additional second ligand system will reveal the chemical and structural potential of the photochemical process. Also, these experiments will establish the complementary information needed for a detailed understanding of the mechanistic pathway. Furthermore, the question of the magnetic ordering behavior within the network of the paramagnetic ions will prompt additional Mössbauer and magnetic susceptibility studies.

Acknowledgment. Gratitude is expressed to the Swiss National Science Foundation for financial support under Project No. 20-27933.89. The authors also thank Professor H. U. Güdel, University of Berne, for stimulating discussions.

Supplementary Material Available: Tables of crystal data and structure determination parameters for **1** and **2** (Table SVIII), hydrogen coordinates and thermal parameters for **1** (Table SIX), bond distances and angles involving hydrogen atoms for **1** (Table SX), anisotropic displacement parameters for **1** (Table SXI), bond distances and angles involving hydrogen atoms for **2** (Table SXII), anisotropic displacement parameters for **2** (Table SXIII), least-squares planes for **1** (Table SXIV), and least-squares planes for **2** (Table SXV) and a figure showing a stereoview of **2** (8 pages). Ordering information is given on any current masthead page.

(23) Zobel, D.; Luger, P.; Dreissig, W.; Koritsanszky, T. *Acta Crystallogr.* **1992**, *B48*, 837.
(24) Wells, A. F. *Structural Inorganic Chemistry*; Clarendon Press: Oxford, England, 1984.
(25) Bancroft, G. M.; Dharmawardena, K. G.; Maddock, A. G. *J. Chem. Soc. A* **1969**, 2914.